Electronic Supplementary Material (ESI) for RSC Advances.

Supplementary Information

Elastic FRET sensors for contactless pressure measurement

Frank Morgner,[ac] Mark Bennemann,‡[a] Piotr J. Cywiński,[a] Matthias Kollosche,[b] Krzysztof Górski,[d] Marek Pietraszkiewicz,[d] André Geßner,*[a] and Hans-Gerd Löhmannsröben[c]

[a] Functional Materials and Devices, Fraunhofer Institute for Applied Polymer Research, Geiselbergstr. 69, 14476 Potsdam-Golm, Germany

[b] Applied Condensed-Matter Physics, Institute of Physics and Astronomy, Faculty of Science, University of Potsdam, Karl-Liebknecht-Str. 24-25, 14476 Potsdam-Golm, Germany

[c] Physical Chemistry, Institute of Chemistry, Faculty of Science, University of Potsdam, Karl-Liebknecht-Str. 24-25, 14476 Potsdam-Golm, Germany

[d] Institute of Physical Chemistry, Polish Academy of Sciences, Kasprzaka 44-52, 01224 Warsaw, Poland.

‡ Currently with Hella KGaA Hueck & Co, Rixbecker Straße 75, 59552 Lippstadt, Germany

* andre.gessner@iap.fraunhofer.de

1. ‘‘Balloon’’ tests with parallel FRET measurements

Fig. S1 sketches the bubble inflation test adapted from [1], [2], [3] and our modifications to characterize the luminescent emission of elastic thin film sensors. This experimental design of the ‘‘Balloon’’ tests, in contrast to uni-axial or pure shear, has the advantage that biaxial stress can be applied in the apex region of the bulge. The elastic sensor allows a direct measurement of the stretch and stress in the apex region. Of course, the deformation and performance of the sensor depends strongly upon the stiffness of the employed materials and the initial thicknesses of the sensor.

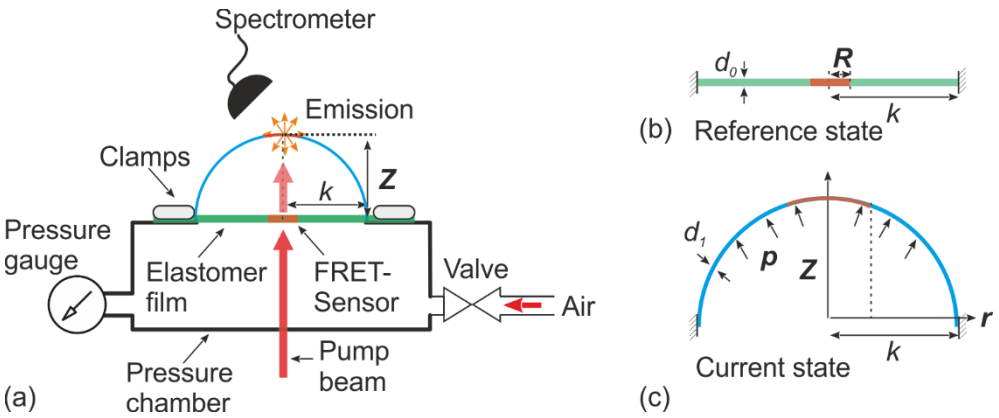

Fig. S1. (a) Schematics of the bubble inflation test with parallel measured luminescence intensities. The soft, stretchable sensor is mounted on a circular aperture with a radius k=10mm and fixed by rigid clamps. The air pressure is manually controlled with a value and monitored with a pressure gauge. The lift Z of the sensor is acquired with a scale in a static inflated state. The excitation laser (pump beam) with a wavelength of 337nm is pointed through the pressure chamber onto the central section of the sensor. The luminescence signal is acquired with a spectrometer targeted on the apex region of the bulge or the central section of the flat film. (b) Cross-section of the elastomer sensor in the initial state with an initial thickness d_0. Due to sensor preparation and mounting processes the elastomer sensor is in a state of small pre-stretch. This initial pre-stretch is conserved by rigid clamps. R corresponds to the radius of the FRET spot. (c) Exposed to a net pressure p the freestanding flat film inflates from a flat state into an axisymmetric shape with a film thickness of d_1.

2. Analytic description of FRET sensor inflation

Beside analytic attempts, finite element (FE) methods are frequently proposed to access the equi-biaxial deformation in dependence of the apex lift Z. A detailed analysis of nonlinear elasticity is beyond the scope of this paper and can be found elsewhere [4], [5], [6]. A rough estimation of apex stretches is required to illustrate the impact of pressure controlled geometry changes and luminescence intensity and FRET of the sensor.

2.1 Experiments on inflated elastomer films

Overall, the geometric responses of SEBS (styrene-ethylene/buthylene-styrene) and PDMS (poly(dimethylsiloxane)) sensors are found to be different if exposed to an identical differential

pressure *p*. To ensure that the sensor film does not exceeds the radius of the orifice (k=Z), *a* suitable pressure level of 20 kPa was set for all inflation experiments. The monitored lift of the SEBS sensor is Z_{SEBS}=4mm while the PDMS sensor show Z_{PDMS}~2mm.

2.2 Luminescence and FRET processes of flat and inflated sensors

During luminescence emission measurements under an alternating net pressure signal ((Off/On) state) the laser spot size is assumed constant. As the elastomer is taken to be incompressible, $L_1L_2L_3$=1, where L_1, L_2, L_3, , are the stretches in the longitudinal, latitudinal, and thickness directions, respectively. The bubble is deformed equi-biaxially in the apex region, such that the acceptor luminescence *I* (without FRET) scales with the thickness as

$$I_{On}/I_{Off} \sim L_3 \qquad \text{(S3)}$$

where I_{On}/I_{Off} is the ratio between the current I_{On} and the initial I_{Off} emission. Fig. S2 plot inflation experiments of the PDMS sensor without FRET processes in the current “On” as well as in the initial “Off” state. The first Off/On variation shows a luminescence intensity ratio of $I_{On,1}/I_{Off,1} = 0.86$ while it is $I_{On,5}/I_{Off,5} = 0.94$ for the 5th cycle (Fig. S2b, acceptor channel). Obviously, the decay of the acceptor intensity over all pressured states is significantly higher compared to all un-pressured Off states. Very similar observations can be made for the timeline of the donor intensities plotted in Fig. S2 a/b.

To compare the luminescence signal changes with pressure induced geometric changes, the apex stretches and thickness stretch L_3 are calculated from experimental readings. The longitudinal stretch of the inflated balloon is defined as $L_1 = b/2k$ where *b* is arc length and *k* the radius of aperture. Based on our evaluation, the inflated PDMS sensor shows an equi-biaxial stretch L_1L_2 in the apex region of $L_{1P,PDMS}$ $L_{2P,PDMS}$ = 1.10x1.10. such that the thickness stretch in the pressured state is $L_{3P,PDMS}$ = 0.82. Within experimental error it seems likely that the thickness stretches scales directly with the intensity ratio of the acceptor signal without FRET.

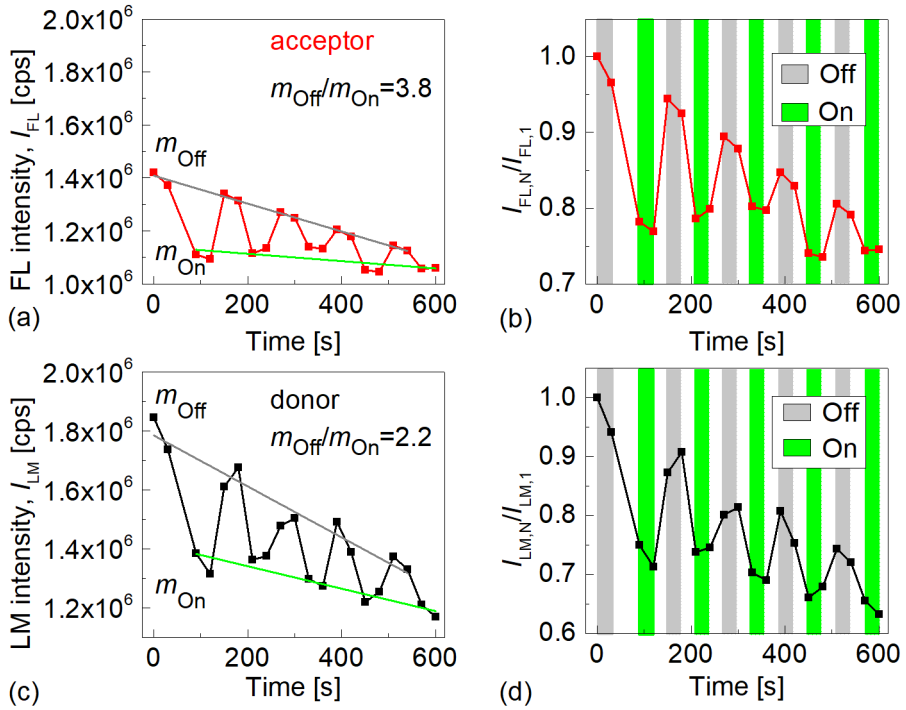

Fig. S2. Luminescence intensity of FRET-pairs lanthanide complex donors/QD acceptors dispersed in PDMS. The sensor is exposed to an alternating Off/On pressure of 20 kPa. The luminescence intensities are measured in equidistant steps as the state is applied and after 30 s before switching states. (a) Luminescence intensity of QD presenting the acceptor channel. The overall decay of pressured and unpressured states is indicated with m_{On} and $m_{Off.}$ (b) Intensity ratio $I_{FL,N}/I_{FL,1}$ of QD acceptors for an alternating On or Off state. The ratio $I_{LM,N}/I_{LM,1}$tends to drift to lower values as the Off/On cycle increases. (c) Signal intensity of LLC- donors including the slope of pressured and unpressured states is indicated with m_{On} and $m_{Off.}$. (d) Intensity ratio I_{On}/I_{Off} of corresponding donor measurements.

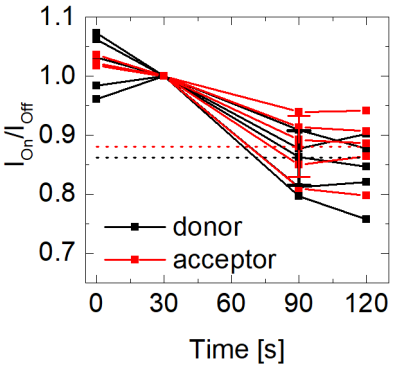

Fig. S3. Normalized acceptor and donor luminescence intensities of the PDMS sensor directly before switching Off/On states. Both the donor and acceptor intensity show a signal decrease and a mean ratio of I_{On} /I_{Off} = 0.86 or 0.88 respectively for the pressured state of the experiment.

In case of FRET but identical deformations, the donor luminescence intensity would give higher readings while the acceptor signal intensity would drop significantly due to a change of the average donor-acceptor-distance. In addition, the lower FRET efficiency causes an increase of donor and a parallel decrease of the acceptor luminescence lifetime.

For the pressured SEBS sensor the inflation lift is Z = 4mm which corresponds to an equi-biaxial stretch of $L_{1P,SEBS}$ $L_{2P,SEBS}$ = 1.45x1.45 and thickness stretch of $L_{3P,SEBS}$ = 0.47.

Nevertheless, luminescence measurements of the inflated SEBS sensor (Fig. 3) shows an intensity ratio of $I_{On,SEBS}/I_{Off,SEBS} \sim 0.65$ for the acceptor signal which is significantly higher than the calculated thickness ratio $L_{3P,SEBS}$. The mismatch between the thickness ratio and the luminescence ratio illustrates that FRET processes contribute to the measured luminescence signal.

2.3 Mechanics of inflated elastomer films

Elastomer films can be stretched in both planar directions L_1L_2 by many times with consequent effect on the thickness direction L_3. For convenience, the elastic sensor is taken to be incompressible $L_1L_2L_3=1$. The current experimental description refers to the observation that the inflation stress σ_I is balanced by suitable hyperelastic stress σ_H. It is assumed that the inflation stress is given as [2], [3]

$$\sigma_H=\sigma_I=p\frac{Z}{2d_0}L_1^2 \tag{S1}$$

where p is the applied pressure, Z the radius of curvature or inflation lift, d_0 the thickness of the unstretched sample and L_1 the axial stretch. A number of materials models such as Mooney–Rivlin, Ogden, Neo Hooke, Yeoh, Arruda–Boyce are available in literature to describe large deformations. In this study and for our convenience we apply the uni-axial Neo-Hookean material model. For an ideal inflated sensor in an apparent stable state, the stress balance read as

$$\frac{Y}{3}\left(L_1^2-\frac{1}{L_1}\right)=p\frac{Z}{2d_0}L_1^2 \tag{S2}$$

Inserting experimental parameters such as the initial thickness, axial lift and applied net pressure into Eq. S1**,** stresses comparable to the tensile experiments (Fig. S3 and Fig. S4) can be determined. Of course, Eq. S2 illustrates that for a constant net pressure p the stretch in the apex region depends directly on the initial film thickness as well as material stiffness Y.

3. Mechanic characterization of elastomer materials

Uniaxial tensile tests are performed on both sets of elastomers (SEBS and PDMS (Sylgard 184)) to obtain material stiffness and creep behaviour under a constant axial stretch. The samples for mechanic tests are prepared as follows. As a first step the liquid elastomers were cast on glass slides and either dried or cured as stated in the document. In a subsequent step, the ready made elastomer films were deselected into uni-axial shaped strips using a laser cutter (Versalaser VLS 2.30). After gently removing the strips from the glass substrate the thickness of each sample was measured at several locations using a micro-meter. In the final step the elastomer strips were clamped into a tensile

tester (Zwick-Roell Z005 equiped either with a 10N and a 100N load cell) and tested acordingly. To allow a statistic evaluation at least 5 subsequent measurements are performed for each strain rate.

3.1 Mechanic testing

Fig. S4 and Fig. S5 report engineering stress stretch/strain measurements on SEBS and PDMS at different strain rates. To match the large stretches of inflated films, a Neo-Hookean material model was fitted to all uni-axial tensile tests in the stretch interval L_1 = 1.00-1.60. The experiments reveal that the material stiffness Y of both elastomers is nearly stretch rate independent. Our analysis shows that PDMS has a stiffness of 1.6 MPa while SEBS has a stiffness of 320 kPa. The small stretch rate impact on the apparent stiffness of the SEBS allows us to neglect viscoelastic contributions in our experiments.

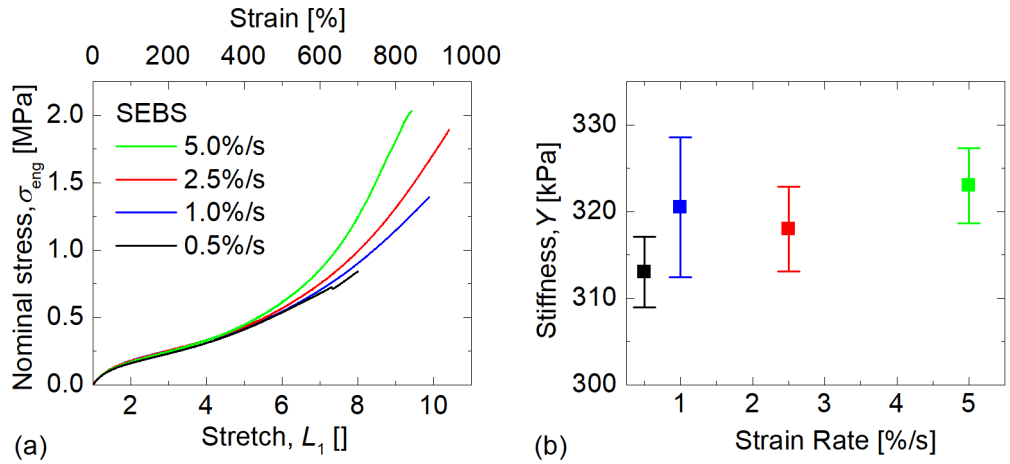

Fig. S4. Uni-axial stress stretch/strain curves of SEBS. (a) Tensile rupture experiments using different strain rates. (b) Mean material stiffness *Y* of 5 independent measures with errors under strain rate variation.

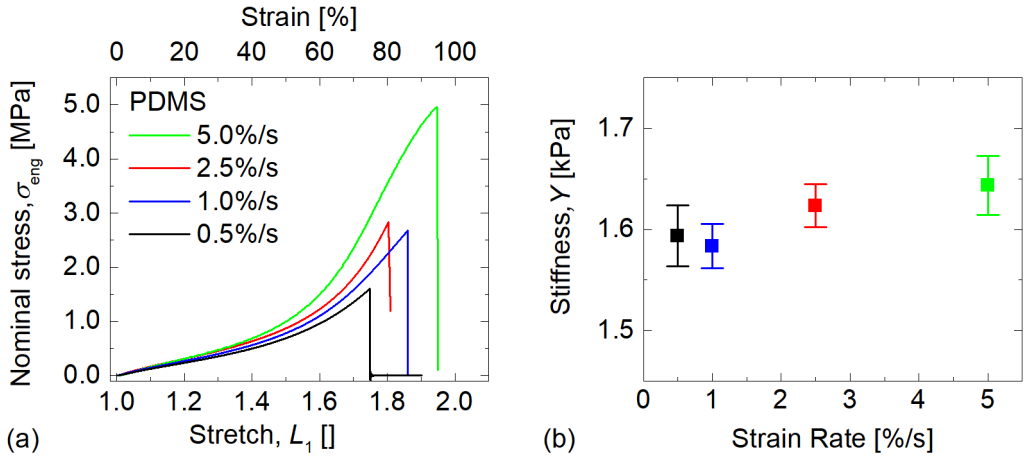

Fig. S5. Uni-axial stress stretch/strain curves of PDMS film (Sylgard 184, Dow Corning). (a) Tensile rupture experiments on virgin samples using different strain rates. **(b)** Mean stiffness *Y* of at least 5 consequent measures under strain rate variation.

Obviously, the ultimate stretch/strain and ultimate stress of PDMS (Fig. S5) depends on the stretch rate. For PDMS the ultimate stretch increase from 1.75 (75%) up to 1.97 (97%) as the strain rate increases from 0.5%/s up to 5%/s. For the softer SEBS, the ultimate stretch is found to be nearly independent from the strain rates which might be due to test conditions.

For stress relaxation experiments the uniaxial samples were stretched from the initial state to a target stretch of either L_{1p}=1.5 (50%) or L_{1p}=2 (100%) using a strain rate of 2.5%/s. Fig. S6 (a) and (b) report the subsequent relaxation phase of 10 min (fixed position). The force data was recorded continuously with a rate of 10 Hz and the force signal of SEBS and PDMS is found to decrease not more than 10% after 600 s. Comparing the relative force change of SEBS as well as the luminescence (I_{FM}) changes for a time step of 30 s after either stretch or pressure is applied shows a relative force change of approx. 2.5% and a change of luminescence of 2.7%. Of course, the creep behavior is strongly affected by stretch and the loading history. Nevertheless, stress relaxation should be considered since creep phenomena of SEBS as well as PDMS are on a comparable time scale (Fig. S6a and Fig. S6a) as the drift of the luminescence and fluorescence intensity as well.

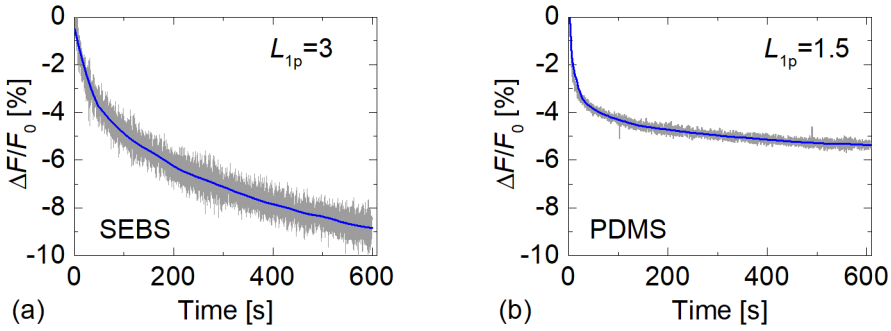

Fig. S6. Force relaxation of stretched SEBS and PDMS. (a) SEBS at L_{1p}=3 stretch (200% strain), (b) PDMS at L_{1p}=1.5 stretch (50% strain). After loading, the initial 30 s of the curve show a force drop of 2.5% and 3.2% for the SEBS and the PDMS respectively.

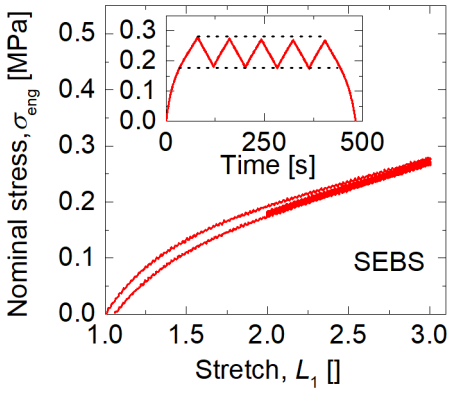

Fig. S7. Cyclic stress stretch curve of SEBS with a strain rate of 2.5%/s and an intermediate cycling between L_1=2 (100%) and L_1=3 (200%). The insert shows the stress time curve and highlights the mechanic reversibility R ~ 97% for cycling between both stretch goals.

REFERENCES

[1] L. R. G. Treloar, Rubber Chem. Technol. **1944**, 17, 957.

[2] N. Reuge, F. M. Schmidt, Y. L. Maoult, M. Rachik, F. Abbe, Polym. Eng. Sci. **2001**, 41, 522.

[3] M. Sasso, G. Palmieri, G. Chiappini, D. Amodio, Polym. Test. **2008**, 27, 995.

[4] L.R.G. Treloar, Trans. Inst. Rubber Ind. **1944**, 19, 201.

[5] Adkins, J. E., and Rivlin, R. S., Philos. Trans. R. Soc. London, Ser. A, **1952**, 244, 505.

[6] Zhu J., Cai S., Suo Z., JMPS **2010**, 24, 3254.